Biophysical Chemistry 307 (2024) 107168

Contents lists available at ScienceDirect

Biophysical Chemistry

journal homepage: www.elsevier.com/locate/biophyschem

On the importance of being amidated: Analysis of the role of the conserved C-terminal amide of amylin in amyloid formation and cytotoxicity

Tangweina Yang [a,1], Ivan Filippov [a,1], Lakshan Manathunga [b,c,1], Aria Baghai [a], Amandine Maréchal [a,d], Daniel P. Raleigh [a,b,c,*], Alexander Zhyvoloup [a,*]

[a] Institute of Structural and Molecular Biology, Division of Biosciences, University College London, Gower Street, London WC1E 6BT, United Kingdom
[b] Laufer Center for Quantitative Biology, Stony Brook University, Nicolls Road, Stony Brook, NY 11790, United States
[c] Department of Chemistry, Stony Brook University, Nicolls Road, Stony Brook, NY 11790, United States
[d] Institute of Structural and Molecular Biology, Division of Biosciences, Birkbeck College, London WC1E 7HX, United Kingdom

ARTICLE INFO

Keywords:
Amidation
Amylin
Amyloid
beta-cells
Diabetes
Islet amyloid polypeptide

ABSTRACT

The polypeptide hormone Amylin (also known as islet amyloid polypeptide) plays a role in regulation of glucose metabolism, but forms pancreatic islet amyloid deposits in type 2 diabetes. The process of islet amyloid formation contributes to β-cell dysfunction and the development of the disease. Amylin is produced as a pro-from and undergoes processing prior to secretion. The mature hormone contains an amidated C-terminus. Analysis of an alignment of vertebrate amylin sequences reveals that the processing signal for amidation is strictly conserved. Furthermore, the enzyme responsible for C-terminal amidation is found in all of these organisms. Comparison of the physiologically relevant amidated form to a variant with a free C-terminus (Amylin-COO^-) shows that replacement of the C-terminal amide with a carboxylate slows, but does not prevent amyloid formation. Pre-fibrillar species produced by both variants are toxic to cultured β-cells, although hAmylin-COO^- is moderately less so. Amyloid fibrils produced by either peptide are not toxic. Prior work (*ACS Pharmacol. Translational. Sci.* 1, 132–49 (2018)) shows that Amylin- COO^- exhibits a 58-fold reduction in activation of the $Amylin_1$ receptor and 20-fold reduction in activation of the $Amylin_3$ receptor. Thus, hAmylin-COO^- exhibits significant toxicity, but significantly reduced activity and offers a reagent for studies which aim to decouple hAmylin's toxic effects from its activity. The different behaviours of free and C-terminal amidated Amylin should be considered when designing systems to produce the polypeptide recombinantly.

1. Introduction

The neuropancreatic hormone Amylin (also known as islet amyloid polypeptide or IAPP) plays a role in energy homeostasis and the regulation of glucose metabolism by contributing to satiety, regulation of gastric emptying and suppression of glucagon release [1–3]. However, human Amylin (hAmylin) is well-known for its high propensity to form amyloid fibrils *in vitro* and *in vivo*. Amyloid formation in the pancreatic islets of Langerhans is a hallmark of type 2 diabetes [1,4–17]. The process of islet amyloid formation by hAmylin contributes to β-cell death and dysfunction in type 2 diabetes (T2D) as well as to the failure of islet transplants [1,7,9,10,13,17–19]. All vertebrates examined to date produce Amylin [20].

Like many polypeptide hormones, the 37-residue C-terminally amidated human Amylin (hAmylin) polypeptide is synthesized as a pro-form (pro-hAmylin) and undergoes processing prior to secretion [21]. In functioning human β-cells, the 37-residue mature form of hAmylin is derived from a 69-residue peptide, pro-peptide. Pro-hAmylin contains

Abbreviations: hAmylin, the mature amidated form of human-amylin; hAmylin-COO^-, the form of hAmylin with a free C-terminus instead of an amidated C-terminus; EC_{50}, the concentration of peptide required to achieve half the maximum effect in a cell viability assay; FTIR, Fourier Transform infrared spectroscopy; PBS, phosphate buffered saline; Pro-Amylin, the pro form of Amylin; SASA, solvent accessible surface area; T_{50}, the time required to reach half the maximum thioflavin-T fluorescent intensity in a kinetic assay; T2D, type-2 diabetes; TEM, transmission electron microscopy..

* Corresponding authors at: Institute of Structural and Molecular Biology, Division of Biosciences, University College London, Gower Street, London WC1E 6BT, United Kingdom; Department of Chemistry, Stony Brook University, Nicolls Road, Stony Brook, New York 11790, United States.
E-mail addresses: daniel.raleigh@stonybrook.edu, d.raleigh@ucl.ac.uk (D.P. Raleigh), a.zhyvoloup@ucl.ac.uk (A. Zhyvoloup).
[1] These Authors contributed equally to this work

https://doi.org/10.1016/j.bpc.2023.107168
Received 3 October 2023; Received in revised form 17 December 2023; Accepted 28 December 2023
Available online 2 January 2024

an 11 residue N-terminal extension and a 21 residue C-terminal extension relative to the mature form of hAmylin. The pro-peptide is processed in a number of steps (Fig. 1). The first involves proteolytic processing at the C-terminus of pairs of dibasic residues (Lys(−1), Arg (−2),) and (Lys52,Arg53), by the prohormone convertases PC 2 and PC 1/3, (Fig. 1) [21–23]. Note here we use numbers chosen so that the N-terminus of the mature form is numbered as residue 1 and residues in the N-terminal extension are numbered, −1, −2, −3 *etc.* Cleavage by the same prohormone convertases is involved in the processing of insulin. Cleavage by PC2 and PC1/3 generates new N- and C-termini and shortens pro-hAmylin to a 40-residue form which differs from mature hAmylin by a Gly-Arg-Arg extension at the C-terminus. While no further processing occurs at the N-terminus, the C-terminus undergoes processing by carboxypeptidase E (CPE) to remove the dibasic prohormone convertase recognition sequence. The resulting polypeptide includes an extra C-terminal glycine residue which acts as the nitrogen donor for the amidation step. This step is catalysed by the peptidyl amidating monooxygenase (PAM) complex and leads to the removal of the $C_\alpha H_2COOH$ subunit of the C-terminal Gly and introduction of an amide functionality at the C-terminus (residue Tyr37) of mature hAmylin. Many biologically active polypeptides are C-terminally amidated. Amidated peptides are less susceptible to proteolytic degradation, and this can extend their half-life in the bloodstream. Amidation can also affect the affinity of peptides to their G-protein coupled receptors.

C-terminal amidation is known to significantly impact receptor activation by hAmylin. There is a family of Amylin receptors, with each consisting of a complex of the calcitonin receptor, a member of the group of small class B GPCRs, and a receptor activity modifying protein (RAMP) [24]. There are three distinct RAMPs which lead to three different amylin receptors. Amylins also bind the calcitonin receptor in the absence of RAMPs, but with reduced affinity. The impact of C-terminal amidation on the activation of the human calcitonin receptor and the human $Amylin_1$ and $Amylin_3$ receptors by hAmylin have been characterized using a cell-based model [25]. Replacement of the C-terminal amide with a carboxylate led to a 58-fold reduction in activation at the $Amylin_1$ receptor and a 20-fold reduction at the $Amylin_3$ receptor. In contrast, mutation of the C-terminal Tyr to Phe or Ala while maintaining the amidated C-terminus leads to much more modest reductions and substitution with a Pro while maintaining the amidated terminus increases receptor activation modestly. The impact of the conversion of the C-terminal amide to a free carboxylate has much more modest effects on calcitonin receptor activation by hAmylin, causing only a 2.6-fold decrease, relative to its effect on Amylin receptors [25]. There are no structure function studies of amylins from different species binding to their natural receptors, so it is not known if this trend is found in other organisms. However, the key observation is that amidation has a major impact on human hAmylin receptor activation.

Less is known about the effect of amidation on hAmylin amyloid and on hAmylin toxicity towards β-cells. It is also not known how widely conserved C-terminal amidation is among vertebrate amylins. Here we conduct a bioinformatics analysis of the conservation of the C-terminal amidation of amylins and the conservation of PAM and we compare the *in vitro* amyloidogenicity and cytotoxicity of the physiologically relevant amidated form to the variant with a free C-terminus.

2. Materials and methods

2.1. Sequence analysis of amylins

Annotated and predicted amylin sequences were collected from NCBI orthologs database, and the protein sequences were aligned using COBALT [26,27]. The resulting alignment of 485 unique sequences (one sequence per gene), belonging to *Gnathostomata* was quality controlled, and 2 sequences lacking any recognisable cleavage signals were removed. Following this, the alignment was manually trimmed in AliView to include three additional residues off the N-terminal and four additional residues off the C-terminal of the mature amylin sequence (defined as sequence flanked by the cleavage signals) [28]. After removing 6 outliers, which differ in the length of the putative mature sequence, a Weblogo diagram was created using WebLogo3, (https://weblogo.berkeley.edu/logo.cgi) and a consensus sequence was calculated using the 479 sequences by EMBOSS Cons with a threshold value of 0 [29–31]. The presence of PAM in each species represented in the alignment was confirmed by a database search of the NCBI genbank.

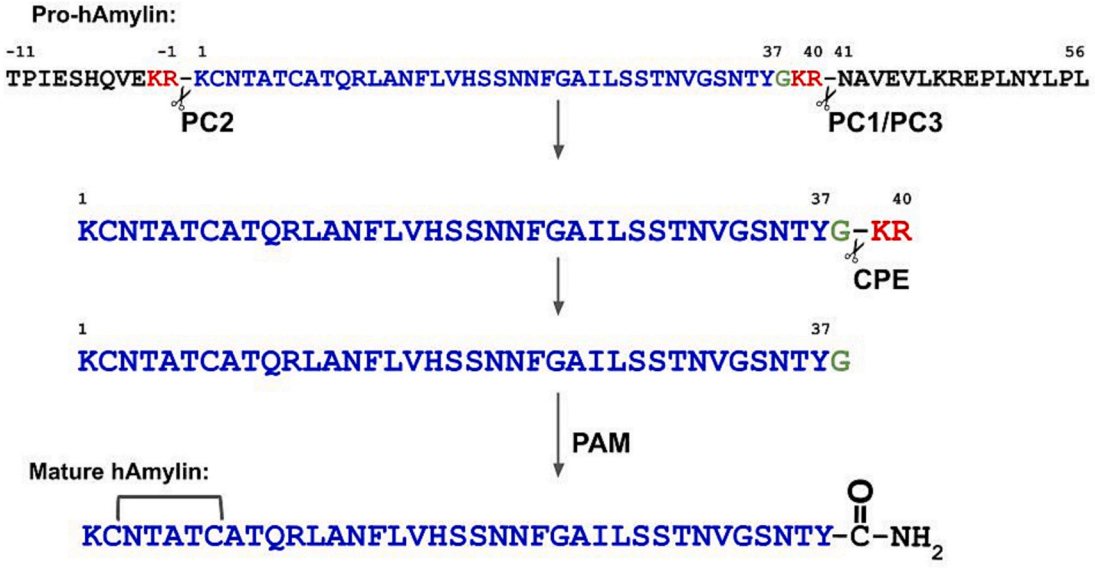

Fig. 1. Schematic representation of the processing of Pro-hAmylin. Prohormone convertases - prohormone 1/3 (PC1/PC3) and prohormone convertase 2 (PC2) cleave the prosequence after a dibasic recognition sequences (highlighted in red). This removes the N-terminal extension completely, but leaves 3 extra residues at the C-terminus. The remaining dibasic sequence at the C-terminus is removed by carboxypeptidase E (CPE). In the final step, peptidylglycine-alpha-amidating monooxygenase (PAM) utilises the C-terminal glycine as a nitrogen donor to form the C-terminal amide. A disulfide bridge is formed between C2 and C7. The numbering here corresponds to the mature sequence, with residues in the N-terminal extension labelled as negative. (For interpretation of the references to colour in this figure legend, the reader is referred to the web version of this article.)

2.2. Materials

hAmylin and hAymlin-COO- were purchased from The ERI Amyloid Laboratory, LLC (Oxford CT, USA).

2.3. Thioflavin-T assays of amyloid formation

Thioflavin-T binding kinetic assays were used to monitor the development of ordered fibrils as a function of time. Thioflavin T assays were conducted on a Beckman Coulter DTX 880 Multimode Detector plate reader and on a BMG Labtech H30–1022 CLARIOstar plater reader. Thioflavin T fluorescence was measured at 430 nm excitation wavelength and 485 nm emission wavelength. Corning 96-well non-binding surface black plates with lids were used for the assays, and the plates were sealed with polyethylene plate sealing tape. Fluorescence intensity was measured from the bottom of the plate. Lyophilized dry peptides were dissolved in PBS buffer at pH 7.4 immediately before the assays. The final experiments were conducted at 25 °C without additional agitation. The concentration of hAymlin and hAmylin-COO- was 25 μM and the concentration of thioflavin-T was 25 μM. Uncertainties are the apparent standard deviation based upon multiple repeats (minimum 3 repeats).

2.4. Transmission electron microscopy (TEM)

10 μL peptide samples were collected at the end of kinetic experiments and were blotted onto a carbon-coated formvar 300 mesh copper grid for 1 min and then negatively stained with 2% depleted uranyl acetate for 1 min for TEM image. TEM images were taken using an FEI TEM microscope at the central microscopy center at the Stony Brook University.

2.5. Attenuated total reflectance Fourier transform infrared (FTIR) spectroscopy of amyloid fibrils

100 micromolar peptide in deuterated PBS was incubated in D_2O for 96 h. The samples were then centrifuged at 21300 RCF for 10 min and the supernatant was removed. Fibril material was removed, placed on the prism of the spectrometer and concentrated by drying with a stream of argon. Spectra were recorded over the range of 3000 to 800 Cm^{-1} and are the average of 500 repeat scans. Infrared spectra were recorded at 4 cm^{-1} resolution in attenuated total reflectance mode using a Bruker Vertex 80v (operated with Bruker OPUS 7.5 software) fitted with a liquid-nitrogen cooled MCT-C detector and a three-reflection silicon microprism with ZnSe optics. Frequencies quoted have an accuracy of $+/-$ 1 Cm^{-1}.

2.6. Cell viability assays and determination of EC_{50} values

Toxic effects of the peptides towards cultured cells were evaluated using rat insulinoma β- INS-1832/13 cells which were purchased from AddexBio (#C0018024) and a viability/metabolic activity assay, CellTiter-Glo® 2.0 (Promega, #G9242). Cells were cultured in optimized RPMI-1640 medium (AddexBio, #C0004–02) supplemented with 10% ultra-low IgG FBS (Gibco, #16250078), Penicillin/Streptomycin antibiotic mixture and 50uM 2-Mercaptoethanol. The assay was run in 96-well format using half-area clear bottom white plates (Greiner, #675083). Plates were seeded at 25×10^3 per well and incubated for 24 h in a 5% CO_2 humidified incubator at 37 °C prior to use. An appropriate quantity of peptide was aliquoted from a HFIP master stock solution and lyophilized. Aliquots were diluted in the complete medium to the final desired concentration and immediately applied to the cells by replacing the old medium. The cells were incubated at the same growing conditions for another 24 h and subjected to the CellTiter-Glo assay according to the manufacturer's protocol. Briefly, the plates were cooled to room temperature and an equal volume of the CellTiter-Glo® 2.0 reagent was added to the cells. Plates were shaken vigorously (700 rpm) for one minute, allowed to stand for 5 additional minutes and the luminescence intensity was measured using a Clariostar plate reader. Four biological experiments testing each condition in triplicate were performed.

To test the effect of preformed amyloid fibrils, samples of 167.5 μM hAmylin and 257 μM hAmylim-COO- were dissolved in FBS free RPMI and incubated for 96 h. The generation of thioflavin-T positive material was confirmed. Aliquots were removed, added to INS-1832/13 cells and the effects on cell viability assessed as described above. Statistical analysis, graphics and determination of EC_{50} values were produced using GraphPad Prism 9.5.1.

3. Results and discussion

3.1. The processing signals for C-terminal amidation of Amylin are strictly conserved among vertebrate amylins

There are several lines of evidence which argue that the C-terminal amidation of Amylins is conserved. We have found that the C-terminal processing signal located within pro-Amylin is strictly conserved and PAM is found in all species which are known to produce Amylin. We first examined the potential conservation of the C-terminal amidation signal by constructing an alignment of 479 sequences which have been annotated as Amylins (Supporting table 1). Amylin sequences were extracted from the NCBI orthologs database. The alignment included the prosequence of IAPP, which is processed by prohormone convertase at the terminal dibasic cleavage signals. We then constructed an alignment 44 residues in length, which included mature amylin and three flanking residues on the N-terminal side and four on the C-terminal side. Thus, the aligned sequence includes both the potential N- and C-terminal cleavage signals and their flanking residue. The standard prohormone convertase cleavage signal of a pair of dibasic residues is highly conserved in the N-terminal extension, although there are a few examples of sequences which have only one basic residue at the N-terminal cleavage site, porcine amylin for example. In contrast, the Gly-Basic-Basic tri-peptide extension located C-terminal to mature amylin is strictly conserved in our alignment, outside of three species of camels featuring a GKG extension. (Fig. 2, Table 1 S1). The C-terminal Glycine is strictly conserved in all sequences. The residue N-terminal to the dibasic cleavage N-terminal sequence and the residue C-terminal to the C-terminal dibasic cleavage sequence are notably less conserved. The enzyme responsible for C-terminal amidation, PAM is present in each species represented in the alignment. Finally, Amylin is a member of the calcitonin superfamily of polypeptides. These include Amylin, CGRP, calcitonin and adrenomedullin which are all believed to have evolved from a common ancestor. All members of this super family which have been examined contain an amidated C-terminus [32].

3.2. The environment of the C-terminus in known structural models of hAmylin amyloid fibrils

There are twelve high resolution models of the hAmylin amyloid fibril; one is based upon crystal structures of small steric zipper peptides derived from the sequence of hAmylin [33] and another is based on constraints derived from solid state NMR studies [34]. The remaining structures are based on Cryo-EM studies of hAmylin [35–38]. Although the different models differ in their details there are many similarities (Fig. 3). All of them are rich in cross β-sheet structure and include two or four stacks of amylin monomers. Each monomer in a stack forms intermolecular backbone hydrogen bonds with the monomers immediately above and below in the same stack and there are no backbone hydrogen bonds between polypeptide chains located within the same layer. The sidechains form interactions with adjacent monomers in the other stack. In the solid-state NMR based model and in the x-ray crystallography based model all 37 residues are defined, but in most of the Cryo-EM models the N-terminal residues 1 to 12 are not well defined. In

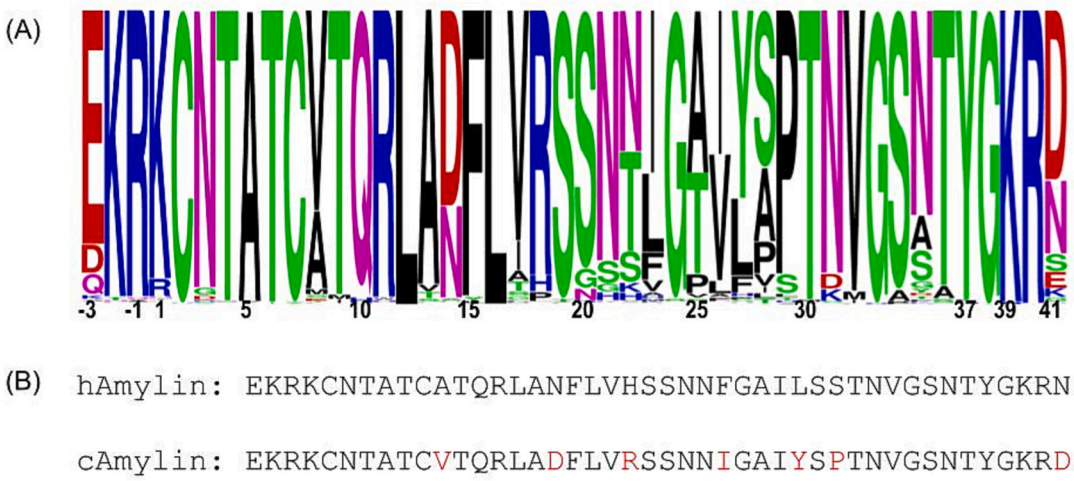

Fig. 2. Conservation of Amylin sequence in vertebrates together with sequence of human amylin and the Amylin vertebrate consensus sequence A) A Weblogo diagram showing the relative frequencies of each residue at each position for mature 37-residue Amylin along with a three residue N-terminal and a four residue C-terminal extension. The numbering used corresponds to the first residue of mature amylin being denote residue-1; B) Comparison of human Amylin (hAmylin) and the consensus Amylin sequence (cAmylin) along with a three residue N-terminal and a four residue C-terminal extension. Residues that differ between the human and consensus sequence are highlighted in red. (For interpretation of the references to colour in this figure legend, the reader is referred to the web version of this article.)

Table 1
% Solvent accessible surface area of the C-terminal amide NH_2 group and the Oxygen-to-Oxygen distance between carbonyl oxygens in the C-terminal amide group in different amylin fibril models. The % SASA is measured relative to an amidated Thr-Tyr-NH_2 dipeptide and the Oxygen-to-Oxygen distance is measured between different monomers in the same stack.

PDB ID	Experimental method	% Avg. Fractional SASA	Y37 carbonyl O to O distance (Å)
(a)	X-ray crystallography of peptide fragments	22.18	5.10
(b) chain a	Solid state NMR	89.40	4.85, 4.93
(b) chain b	Solid state NMR	78.00	5.84, 4.60
6Y1A	Cryo-EM	6.94	4.87
6ZRF	Cryo-EM	20.71	4.91
7M61 - chain a	Cryo-EM	67.73	4.92
7M61 - chain b	Cryo-EM	45.11	4.96
7M62	Cryo-EM	0.00	4.81
7M64	Cryo-EM	10.24	4.85
7M65 - chain a	Cryo-EM	18.91	4.92
7M65 - chain b	Cryo-EM	N/A	4.96
7YKW - chain a	Cryo-EM	0.00	4.74
7YKW - chain b	Cryo-EM	91.98	4.76
7YLO - chain s	Cryo-EM	31.50	4.68
7YLO - chain l	Cryo-EM	91.08	4.74

(a) PDB structure provided by Prof. David Eisenberg (b) PDB structure provided by Dr. Robert Tycko.
(b) contains different monomers within each stack; each chain has two different distances.
Chains a, b refer to asymmetric stacks in fibril structures with two stacks.
Chains s, l refer to the two short and two long stacks in the 7YLO fibril structure that has four stacks.

the Cryo-EM model 7 M62 (Fig. 3 G, H) and in one stack of 7 M65 (Fig. 3 K, L) only the first 5 residues are undefined. In the other stack of this model (Fig. 3 K, L) the first 13 residues and residue 37 are not defined. In the most recent models deduced from Cryo-EM studies (Fig. 3 M, N) one stack contains all 37 residues and in the other stack the first 10 residues are undefined. The other polymorph described in this study (Fig. 3 O, P) contains four stacks. In two of the stacks all 37 residues are defined and in the other two stacks the first 10 residues remain undefined. There is considerable variability in the accessibility of the C-terminal amide group in the various structures. The % solvent accessible surface area (SASA) of the C-terminal NH_2 group, calculated relative to an amidated dipeptide (Thr-Tyr-NH2), ranges from to 91% to 0% (Table 1). However, the majority of the Cryo-EM structures have % SASA values below 50%, indicating at least partial burial of the C-terminal amide group.

Owing to the parallel in register architecture of the β-strands in hAmylin amyloid fibrils, the C-terminus of one chain is close in space to the C-terminus of the chains immediately above and below. The O-to-O distance between carbonyl groups in the C-terminal amide unit ranges from 4.68 to 5.84 Å (Table 1) and all but two of the distances are below 4.96 Å. This indicates that significant electrostatic repulsion would result if the fibrils formed by hAmylin-COO^- adopted the same structure as those formed by the amidated polypeptide. Of course, binding of counter ions could lead to significant screening of electrostatic repulsion and the highly polymorphic nature of hAmylin amyloid fibrils suggests that the two polypeptides do not have to form the same fibril structure.

3.3. Conversation of the C-terminal amide to a carboxylate slows, but does not eliminate amyloid formation in vitro

We next examined the effect on the kinetics of amyloid formation caused by replacing the C-terminal amide with a carboxylate The substitution could lead to electrostatic repulsion between the termini as noted above, which might slow amyloid formation. On the other hand, the introduction of a free C-terminal carboxylate in place of the C-terminal amide will reduce the overall net charge on the polypeptide which might promote aggregation, thus it is difficult to predict the effects. We used thioflavin-T assays to follow the kinetics of amyloid formation. Thioflavin-T is a small molecule which is weakly fluorescent in solution, but its quantum yield increases dramatically when it binds to amyloid fibrils. Thioflavin-T is thought to bind in groves formed by the in-register rows of solvent exposed sidechains on the amyloid fibrils surface [39,40]. Thioflavin-T accurately reports on the time course of hAmylin amyloid formation [41] under the conditions of our experiments, but there are reports of *in vitro* amyloid fibrils formed from a non-human Amylin which do not bind thioflavin-T [42]. We confirmed the presence of amyloid fibrils *via* transmission electron microscopy (TEM).

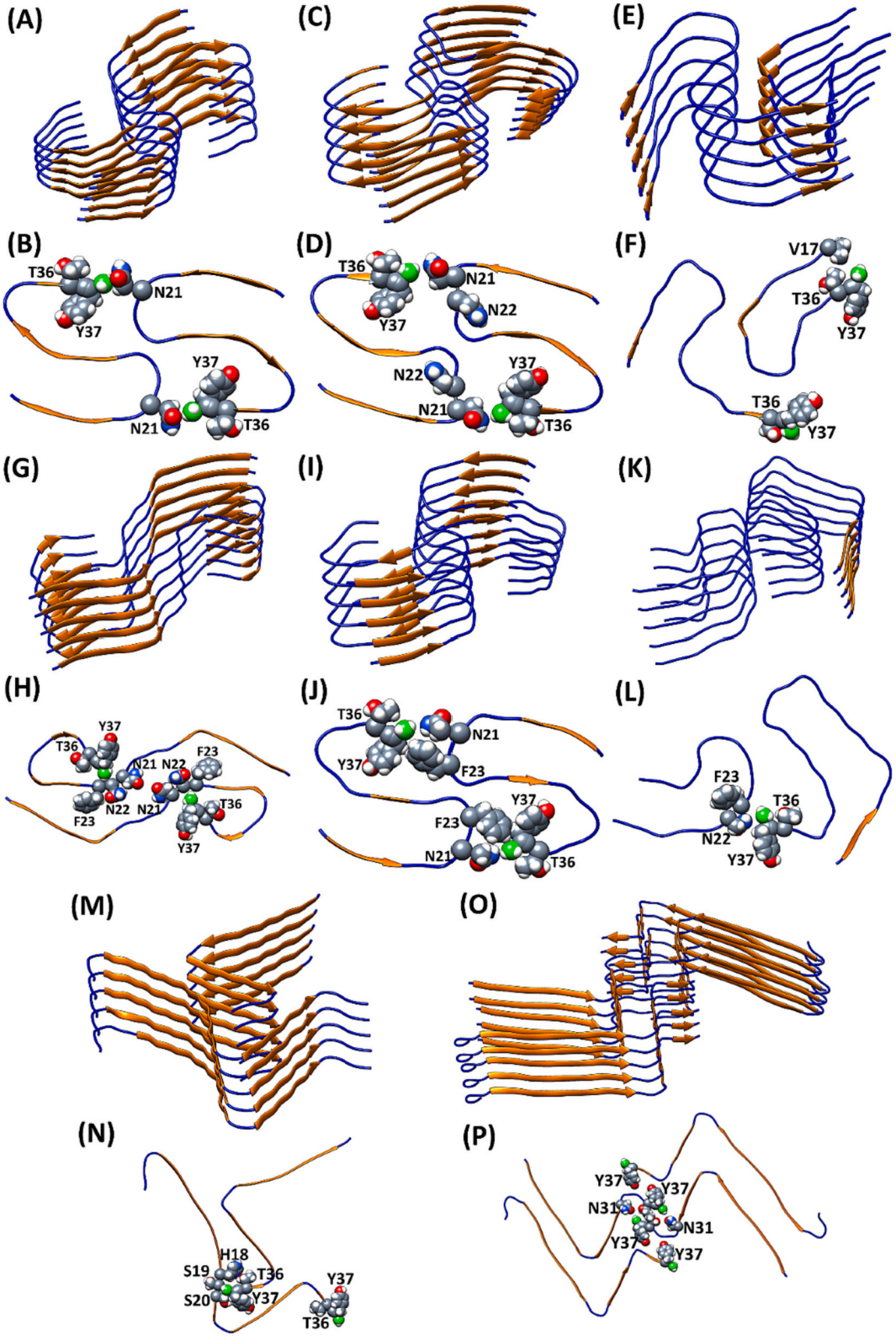

Fig. 3. The position of the amidated C-terminus and its surrounding atoms in different hAmylin fibril models. Each model is illustrated as ribbon diagrams and a top-down cross-sectional view of each fibril model is displayed immediately below each ribbon diagram. The atoms of Tyr37 and residues around it are illustrated as spheres where grey indicates Carbon atoms, white indicates Hydrogen atoms, red indicates Oxygen atoms, blue indicates Nitrogen atoms and green indicates the Nitrogen atom of the C-terminal amide group. All of the fibril models illustrated here are derived from Cryo-EM studies of: (A,B) synthetic IAPP conducted at pH = 6.0 (PDB = 6Y1A); (C,D) synthetic IAPP conducted at pH = 6.8 (PDB = 6ZRF); (*E*-L) samples seeded by human tissue extracts (PDB = 7 M61, 7 M62, 7 M64, 7 M65); (M-P) synthetic IAPP in Milli-Q water (PDB = 7YKW, 7YL0). The Cryo-EM structures contain only the residues that fall in the ordered region and the C-terminal Tyrosine residue in one stack of the Cryo-EM model (*K*,*L*) is not included. All of the other structures contain the C-terminal Tyrosine.

hAmylin-COO- formed amyloid more slowly than the amidated form in phosphate buffered saline (PBS) (Fig. 4, Fig. S1). The T_{50}, the time at which 50% of the total signal change in a thioflavin-T assay has occurred, increased by a factor of slightly larger more than 4-fold. We found some variation in the exact T_{50} values depending upon the plate reader used, (likely because of different amounts of agitation when the plates are moved for sampling) and depending on the total sample volume used. However, the key point is that hAmylin-COO- was always slower to form amyloid than normal hAmylin, and the effects, while significant, were relatively modest. These experiments were performed at 25 °C. We repeated the measurements at 37 °C. As expected, amyloid formation by both peptides is more rapid at the higher temperature (Fig. S2), but the same trend is observed with hAmylin-COO- forming amyloid more slowly than normal hAmylin. The T_{50} values differs by a factor of close to 6 at 37 °C, under the conditions of our studies.

TEM images of samples collected at the end of the kinetic curves shown in Fig. 4 were recorded to confirm the presence of fibrils. Dense matts of fibrils were observed for both polypeptides and no obvious differences were detected at the limited resolution of the TEM measurements.

We also collected attenuated total reflectance FTIR spectra of the amyloid fibrils formed by the two polypeptides in order to test for any potential differences in secondary structure. The spectra were virtually superimposable and the amide—I band of each sample has a maximum in the range of 1622 to 1624 Cm^{-1}, indicating significant β-sheet content for both sets of amyloid fibrils. The spectra are consistent with published FTIR spectra of amyloid fibrils formed by hAmylin (Fig. S3).

Although beyond the scope of this work, Cryo-Em Studies of hAmylin-COO- would be interesting and would indicate how the additional charged group is accommodated into the fibril structure.

3.4. Conversation of the C-terminal amide to a carboxylate modestly reduces in vitro toxicity towards cultured β-cells

We next compared the effect of the two polypeptides on cell viability using the INS-1832/13 rat insulinoma β-cell line. Cell viability was followed by monitoring cellular ATP production (Fig. 5). The EC_{50} for Amylin was found to be 62.7 to 65.5 μM (95% confidence limits) and the value for hAmylin-COO- was measured to be 94.4 to 105.6 μM (95% confidence limit). This is a small effect and is less than has been observed for a number of point mutants, although there are other point mutants which have no impact on toxicity [41].

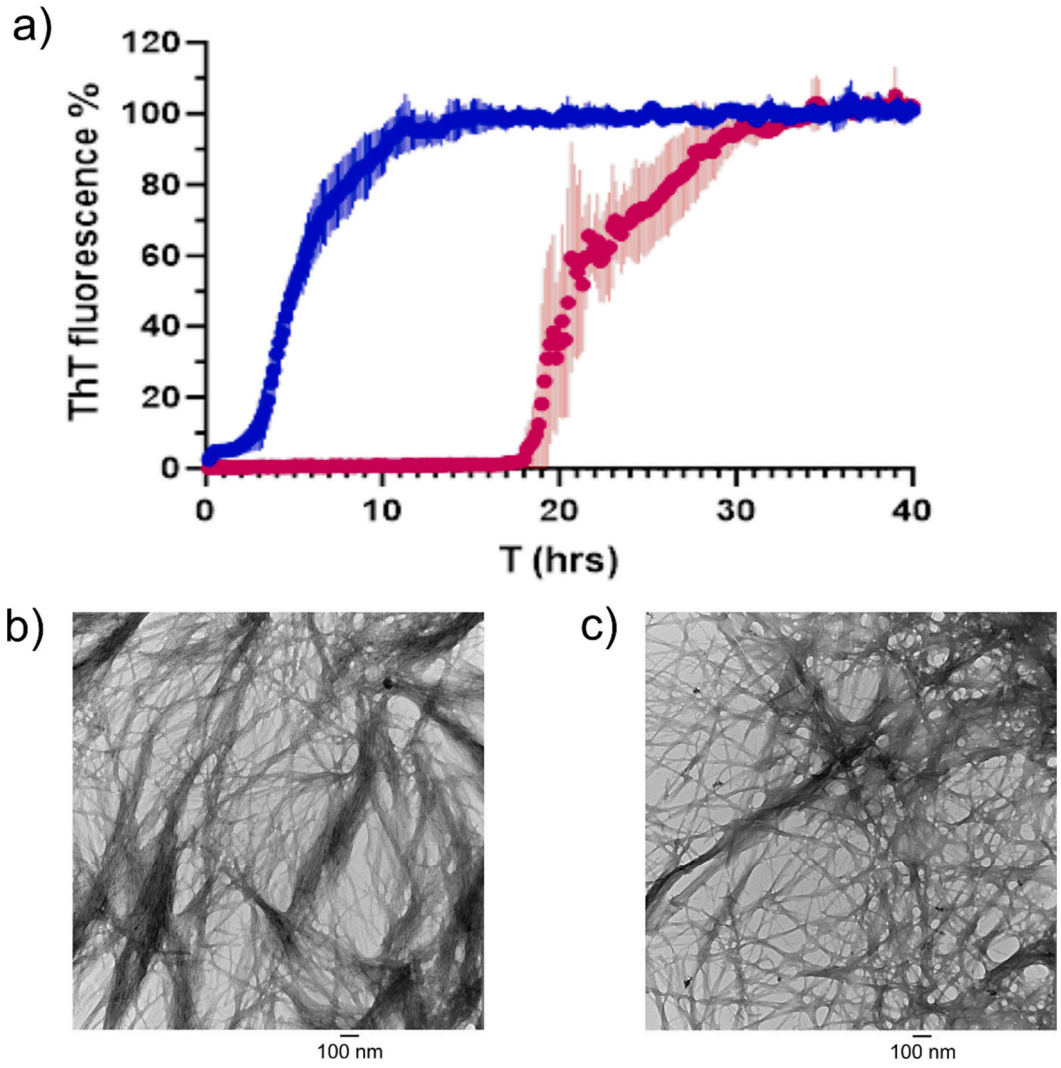

Fig. 4. Comparison of kinetics of amyloid formation between hAmylin and hAmylin-COO- measured at 25 °C in PBS pH 7.4. A) Thioflavin-T kinetic data for hAmylin (Blue) and hAmylin-COO- (Magenta). The curves are normalized on the Y-axis from 0 to 100. The unnormalized data is shown in the supplementary data (Fig. S1). B) TEM image of hAmylin fibrils collected at the end of the kinetic curve. C) TEM image of hAmylin-COO- fibrils collected at the end of the kinetic curve.

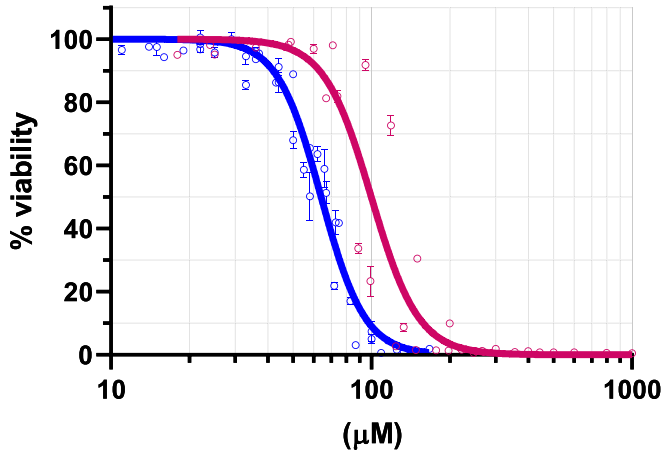

Fig. 5. Replacement of the C-terminal amide group with a carboxylate has only a modest effect on cytotoxicity. Dose-dependent viability of INS-1832/13 cells as monitored by effects on cellular ATP production. Cells were treated for 24 h with increasing concentrations of hAmylin (Blue) or hAmylin-C00- (Magenta) peptides. Cellular ATP production was monitored using the CellTiter-GLO assay. The primary data was normalized to the average viability of the untreated cells. The dose-dependent sigmoid toxicity curves were built using Prism 9.5.1 using normalized primary data from four independent experiments performed in triplicate. The error bars represent the SEM of the normalized averages. (For interpretation of the references to colour in this figure legend, the reader is referred to the web version of this article.)

hAmylin fibrils have been shown to be non-toxic to cultured β-cells [10], but the effect of hAmylin-COO- amyloid fibrils on cell viability has not been examined. Consequently, we tested the effect of hAmylin-COO- amyloid fibrils on cell viability. hAmylin and hAmylin-COO- were incubated at high concentration for 96 h to allow fibril formation and then applied to cultured INS-1832/13 cells. No loss of cell viability was observed in contrast to the significant effects observed for pre-fibril species (Fig. S4).

4. Conclusions

The processing signals for C-terminal amidation are strictly conversed in all vertebrate Amylins examined in our alignment and the amidating enzyme complex (PAM) is found in all of these species. These observations strongly argue that C-terminal amidation is a conserved feature of vertebrate amylins. Along these lines, hAmylin is a member of the calcitonin peptide superfamily and the human sequences in this superfamily are all C-terminally amidated.

Replacement of the physiologically relevant C-terminal amide with a carboxylate lead to a longer time to form amyloid and a modest decrease in toxicity. Prior studies have shown that conversion of the C-terminal amide to a carboxylate leads to a significant effect on receptor activation. A 58-fold reduction in activation at the Amylin-1 receptor (AMY_1) and a 20-fold reduction at the AMY_3 receptor were reported and this is much more significant than the effects observed upon mutating the sidechain to Ala or even Pro [25]. Conversion of the C-terminal amide to a free carboxylate has much more modest effects on calcitonin receptor (CTR) activation by hAmylin leading to a 2.6-fold decrease. The combined effects lead to a reduction in specificity of hAmylin-COO- for the AMY_1 and AMY_3 receptors relative to the calcitonin receptor.

hAmylin-COO^- exhibits significant toxicity, but significantly reduced activity and hence offers a reagent for studies which aim to decouple Amylin's toxic effects from its receptor mediated activity. The different behaviours of the free and C-terminal amidated amylin should be considered when designing systems to produce the polypeptide recombinantly and when designing variants of hAmylin for potential therapeutic applications.

Funding sources

This work was supported by US NIH grant GM078114 and by Wellcome Trust Award 107927/Z/15/Z and by Medical Research Council UK (Transition Support MR/T032154/1).

CRediT authorship contribution statement

Tangweina Yang: Data curation, Methodology, Visualization, Writing – review & editing. **Ivan Filippov:** Data curation, Formal analysis, Investigation, Methodology, Resources, Writing – review & editing. **Lakshan Manathunga:** Formal analysis, Investigation, Visualization, Writing – review & editing. **Aria Baghai:** Data curation, Formal analysis, Investigation. **Amandine Maréchal:** Data curation, Funding acquisition, Methodology, Visualization, Writing – review & editing. **Daniel P. Raleigh:** Conceptualization, Formal analysis, Funding acquisition, Project administration, Supervision, Validation, Visualization, Writing – original draft, Writing – review & editing. **Alexander Zhyvoloup:** Conceptualization, Data curation, Formal analysis, Investigation, Methodology, Project administration, Supervision, Validation, Visualization, Writing – original draft, Writing – review & editing.

Declaration of competing interest

The authors declare they have no known competing financial or personal relationships that could have appeared to influence the work reported in this paper.

Data availability

Data will be made available on request.

Acknowledgments

The authors acknowledge discussions with Ms. Min Hu.

Appendix A. Supplementary data

Supplementary data including one figure which displays the non-normalized thioflavin-T monitored kinetic curves for the two polypeptides, a second figure which displays normalized thioflavin-T monitored kinetic curves for the two polypeptides collected at 37 °C, a third figure showing FTIR spectra of the amyloid fibrils formed by each polypeptide and a table listing all of the sequences used to generate the alignment. Supplementary data to this article can be found online at [https://doi.org/10.1016/j.bpc.2023.107168].

References

[1] P. Westermark, A. Andersson, G.T. Westermark, Islet amyloid polypeptide, islet amyloid, and diabetes mellitus, Physiol. Rev. 91 (2011) 795–826, https://doi.org/10.1152/physrev.00042.2009.
[2] T.A. Lutz, The role of amylin in the control of energy homeostasis, Am. J. Phys. Regul. Integr. Comp. Phys. 298 (2010) R1475–R1484.
[3] R. Akter, P. Cao, H. Noor, Z. Ridgway, L.-H. Tu, H. Wang, A.G. Wong, X. Zhang, A. Abedini, A.M. Schmidt, D.P. Raleigh, Islet amyloid polypeptide: structure, function, and pathophysiology, J. Diabetes Res. 2016 (2016) 2798269.
[4] E.L, Opie on the relation of chronic interstitial pancreatitis to the islands of langerhans and to diabetes melutus, J. Exp. Med. 5 (1901) 397–428.
[5] P. Westermark, C. Wernstedt, E. Wilander, D.W. Hayden, T.D. O'Brien, K. H. Johnson, Amyloid fibrils in human insulinoma and islets of Langerhans of the diabetic cat are derived from a neuropeptide-like protein also present in normal islet cells, Proc. Natl. Acad. Sci. 84 (1987) 3881–3885.
[6] G.J. Cooper, A.C. Willis, A. Clark, R.C. Turner, R.B. Sim, K.B. Reid, Purification and characterization of a peptide from amyloid-rich pancreases of type 2 diabetic patients, Proc. Natl. Acad. Sci. 84 (1987) 8628–8632.
[7] A. Lorenzo, B. Razzaboni, G.C. Weir, B.A. Yankner, Pancreatic islet cell toxicity of amylin associated with type-2 diabetes mellitus, Nature 368 (1994) 756–760.
[8] A. Kapurniotu, Amyloidogenicity and cytotoxicity of islet amyloid polypeptide, Biopolymers 60 (2001) 438-459.

[9] S.E. Kahn, S. Zraika, K.M. Utzschneider, R.L. Hull, The beta cell lesion in type 2 diabetes: there has to be a primary functional abnormality, Diabetologia 52 (2009) 1003–1012.
[10] A. Abedini, A. Plesner, P. Cao, Z. Ridgway, J. Zhang, L.H. Tu, C.T. Middleton, B. Chao, D.J. Sartori, F. Meng, H. Wang, A.G. Wong, M.T. Zanni, C.B. Verchere, D. P. Raleigh, A.M. Schmidt, Time-resolved studies define the nature of toxic IAPP intermediates, providing insight for anti-amyloidosis therapeutics, Elife 5 (2016) e12977.
[11] D. Raleigh, X. Zhang, B. Hastoy, A. Clark, The beta-cell assassin: IAPP cytotoxicity, J. Mol. Endocrinol. 59 (2017) R121–R140.
[12] A. Abedini, A.M. Schmidt, Mechanisms of islet amyloidosis toxicity in type 2 diabetes, FEBS Lett. 587 (2013) 1119–1127.
[13] R.L. Hull, G.T. Westermark, P. Westermark, S.E. Kahn, Islet amyloid: a critical entity in the pathogenesis of type 2 diabetes, J. Clin. Endocrinol. Metab. 89 (2004) 3629–3643.
[14] A. Abedini, J. Derk, A.M. Schmidt, The receptor for advanced glycation endproducts is a mediator of toxicity by IAPP and other proteotoxic aggregates: establishing and exploiting common ground for novel amyloidosis therapies, Protein Sci. 27 (2018) 1166–1180.
[15] M. Blencowe, A. Furterer, Q. Wang, F. Gao, M. Rosenberger, L. Pei, H. Nomoto, A. M. Mawla, M.O. Huising, G. Coppola, X. Yang, P.C. Butler, T. Gurlo, IAPP-induced beta cell stress recapitulates the islet transcriptome in type 2 diabetes, Diabetologia 65 (2022) 173–187.
[16] A. Clark, S.B. Charge, M.K. Badman, E.J. de Koning, Islet amyloid in type 2 (non-insulin-dependent) diabetes, APMIS 104 (1996) 12–18, https://doi.org/10.1111/j.1699-0463.1996.tb00680.x.
[17] G.T. Westermark, P. Westermark, C. Berne, O. Korsgren, T. Nordic, Network for clinical islet, widespread amyloid deposition in transplanted human pancreatic islets, N. Engl. J. Med. 359 (2008) 977–997.
[18] J. Udayasankar, K. Kodama, R.L. Hull, S. Zraika, K. Aston-Mourney, S. L. Subramanian, J. Tong, M.V. Faulenbach, J. Vidal, S.E. Kahn, Amyloid formation results in recurrence of hyperglycaemia following transplantation of human IAPP transgenic mouse islets, Diabetologia 52 (2009) 145–153.
[19] K.J. Potter, A. Abedini, P. Marek, A.M. Klimek, S. Butterworth, M. Driscoll, R. Baker, M.R. Nilsson, G.L. Warnock, J. Oberholzer, S. Bertera, M. Trucco, G. S. Korbutt, P.E. Fraser, D.P. Raleigh, C.B. Verchere, Islet amyloid deposition limits the viability of human islet grafts but not porcine islet grafts, Proc. Natl. Acad. Sci. U. S. A. 107 (2010) 4305–4310.
[20] D. Noh, R.L. Bower, D.L. Hay, A. Zhyvoloup, D.P. Raleigh, Analysis of amylin consensus sequences suggests that human amylin is not optimized to minimize amyloid formation and provides clues to factors that modulate amyloidogenicity, ACS Chem. Biol. 15 (2020) 1408–1416.
[21] T. Sanke, G.I. Bell, C. Sample, A.H. Rubenstein, D.F. Steiner, An islet amyloid peptide is derived from an 89-amino acid precursor by proteolytic processing, J. Biol. Chem. 263 (1988) 17243–17246.
[22] L. Marzban, G. Trigo-Gonzalez, X. Zhu, C.J. Rhodes, P.A. Halban, D.F. Steiner, C. B. Verchere, Role of beta-cell prohormone convertase (PC)1/3 in processing of pro-islet amyloid polypeptide, Diabetes 53 (2004) 141–148.
[23] L. Marzban, G. Trigo-Gonzalez, C.B. Verchere, Processing of pro-islet amyloid polypeptide in the constitutive and regulated secretory pathways of beta cells, Mol. Endocrinol. 19 (2005) 2154–2163.
[24] R.L. Bower, D.L. Hay, Amylin structure-function relationships and receptor pharmacology: implications for amylin mimetic drug development, Br. J. Pharmacol. 173 (2016), 1883-1898. 1.
[25] R.L. Bower, L. Yule, T.A. Rees, G. Deganutti, E.R. Hendrikse, P.W.R. Harris, R. Kowalczyk, Z. Ridgway, A.G. Wong, K. Swierkula, D.P. Raleigh, A.A. Pioszak, M. A. Brimble, C.A. Reynolds, C.S. Walker, D.L. Hay, Molecular signature for receptor engagement in the metabolic peptide hormone amylin, ACS Pharmacol. Transl. Sci. 1 (2018) 32–49.
[26] E.W. Sayers, E.E. Bolton, J.R. Brister, K. Canese, J. Chan, D.C. Comeau, R. Connor, K. Funk, C. Kelly, S. Kim, T. Madej, A. Marchler-Bauer, C. Lanczycki, S. Lathrop, Z. Lu, F. Thibaud-Nissen, T. Murphy, L. Phan, Y. Skripchenko, T. Tse, J. Wang, R. Williams, B.W. Trawick, K.D. Pruitt, S.T. Sherry, Database resources of the national center for biotechnology information, Nucleic Acids Res. 50 (2022) D20–D26.
[27] J.S. Papadopoulos, R. Agarwala, COBALT: constraint-based alignment tool for multiple protein sequences, Bioinformatics 23 (2007) 1073–1079.
[28] A. Larsson, AliView: a fast and lightweight alignment viewer and editor for large datasets, Bioinformatics 30 (2014) 3276–3278.
[29] G.E. Crooks, G. Hon, J.M. Chandonia, S.E. Brenner, WebLogo: a sequence logo generator, Genome Res. 14 (2004) 1188–1190.
[30] T.D. Schneider, R.M. Stephens, Sequence logos: a new way to display consensus sequences, Nucleic Acids Res. 18 (1990) 6097–6100.
[31] P. Rice, I. Longden, A. Bleasby, EMBOSS: the European molecular biology open software suite, Trends Genet. 16 (2000) 276–277.
[32] S.J. Wimalawansa, Amylin, calcitonin gene-related peptide, calcitonin, and adrenomedullin: a peptide superfamily, Crit. Rev. Neurobiol. 11 (1997) 167–239.
[33] J.J. Wiltzius, S.A. Sievers, M.R. Sawaya, D. Cascio, D. Popov, C. Riekel, D. Eisenberg, Atomic structure of the cross-beta spine of islet amyloid polypeptide (amylin), Protein Sci. 17 (2008) 1467–1474.
[34] S. Luca, W.M. Yau, R. Leapman, R. Tycko, Peptide conformation and supramolecular organization in amylin fibrils: constraints from solid-state NMR, Biochemistry 46 (2007) 13505–13522.
[35] C. Roder, T. Kupreichyk, L. Gremer, L.U. Schafer, K.R. Pothula, R.B.G. Ravelli, D. Willbold, W. Hoyer, G.F. Schroder, Cryo-EM structure of islet amyloid polypeptide fibrils reveals similarities with amyloid-beta fibrils, Nat. Struct. Mol. Biol. 27 (2020) 660–667.
[36] R. Gallardo, M.G. Iadanza, Y. Xu, G.R. Heath, R. Foster, S.E. Radford, N.A. Ranson, Fibril structures of diabetes-related amylin variants reveal a basis for surface-templated assembly, Nat. Struct. Mol. Biol. 27 (2020), 1048-1056. 1.
[37] Q. Cao, D.R. Boyer, M.R. Sawaya, R. Abskharon, L. Saelices, B.A. Nguyen, J. Lu, K. A. Murray, F. Kandeel, D.S. Eisenberg, Cryo-EM structures of hIAPP fibrils seeded by patient-extracted fibrils reveal new polymorphs and conserved fibril cores, Nat. Struct. Mol. Biol. 28 (2021) 724–730.
[38] D. Li, X. Zhang, Y. Wang, H. Zhang, K. Song, K. Bao, P. Zhu, A new polymorphism of human amylin fibrils with similar protofilaments and a conserved core, iScience 25 (2022) 105705.
[39] K. Gade Malmos, L.M. Blancas-Mejia, B. Weber, J. Buchner, M. Ramirez-Alvarado, H. Naiki, D. Otzen, ThT 101: a primer on the use of thioflavin T to investigate amyloid formation, Amyloid 24 (2017) 1–16.
[40] H. LeVine, [18] Quantification of β-Sheet Amyloid Fibril Structures with Thioflavin T, Methods in Enzymology 309, Academic Press, 1999, pp. 274–284.
[41] Z. Ridgway, C. Eldrid, A. Zhyvoloup, A. Ben-Younis, D. Noh, K. Thalassinos, D. P. Raleigh, Analysis of proline substitutions reveals the plasticity and sequence sensitivity of human IAPP amyloidogenicity and toxicity, Biochemistry 59 (2020) 742–754.
[42] A.G. Wong, C. Wu, E. Hannaberry, M.D. Watson, J.E. Shea, D.P. Raleigh, Analysis of the amyloidogenic potential of pufferfish (takifugu rubripes) islet amyloid polypeptide highlights the limitations of thioflavin-t assays and the difficulties in defining amyloidogenicity, Biochemistry 55 (2016) 510–518.